Two-neutrino double β decay of deformed nuclei within the quasiparticle random-phase approximation with a realistic interaction

Mohamed Saleh Yousef, Vadim Rodin,[*] Amand Faessler, and Fedor Šimkovic[†]

Institute für Theoretische Physik der Universität Tübingen, D-72076 Tübingen, Germany
(Received 10 June 2008; revised manuscript received 9 December 2008; published 28 January 2009)

A method to implement a realistic nucleon-nucleon residual interaction based on the Brueckner G matrix (for the Bonn-CD force) into the quasiparticle random phase approximation (QRPA) for deformed nuclei is formulated. The two-neutrino double β decay for ground state to ground state transitions $^{76}\text{Ge} \to {}^{76}\text{Se}$ and $^{150}\text{Nd} \to {}^{150}\text{Sm}$ is calculated along with the Gamow-Teller strength distributions. The effect of deformation on the observables is studied.

I. INTRODUCTION

Nuclear double β decay is a second-order weak interaction process that can proceed in two different modes: the two neutrino mode $2\nu\beta\beta$, with the emission of two neutrinos and two electrons, and the neutrinoless mode $0\nu\beta\beta$, with emission of two electrons only, without neutrino emission (see, e.g., Refs. [1–4]). Observation of the latter mode that violates lepton number conservation will prove that the neutrino is a massive Majorana particle.

Theoretical interpretation of electroweak processes in nuclei requires an accurate description of nuclear many-body wave functions. The proton-neutron quasiparticle random phase approximation (QRPA), first considered in Ref. [5], is one of the most reliable nuclear structure methods used for describing the structure of the intermediate nuclear states virtually excited in double β decay. Important ground-state correlations are naturally accounted for within the QRPA as well (see, e.g., Refs. [3,4,6]). The method has been shown to be capable of successfully describing double β decay provided one includes the particle-particle (p-p) residual interaction, along with the usual particle-hole (p-h) one [7]. However, the calculated nuclear matrix elements for double β decay, both the two-neutrino and neutrinoless modes, have been proven to sensitively depend on the parameter g_{pp}, which renormalizes the G-matrix strength in the p-p channel [3,6].

As the majority of $\beta\beta$-decaying nuclei are nearly spherical, spherical symmetry has been assumed in all QRPA calculations of the $0\nu\beta\beta$-decay matrix elements $M^{0\nu}$ up to now. Nowadays, there is a growing interest in the scientific community in double β decay of ^{150}Nd as a very promising candidate for the next generation of experimental searches for the neutrinoless double β decay (SNO+ [8] and SuperNEMO [9]). The nucleus is well known to have one of the largest values of the lepton phase space factor (about 33 times larger than that for ^{76}Ge; see, e.g. Ref. [1]), but it is at the same time strongly deformed, which provides a great obstacle

for reliable theoretical analysis of the corresponding matrix element $M^{0\nu}$. The effect of deformation on the $0\nu\beta\beta$ decay of ^{150}Nd to the ground and excited states of ^{150}Sm was first studied in Ref. [10] within the pseudo-SU(3) model, which is a tractable shell model for deformed nuclei, in which, however, a severely truncated single-particle basis is used. The matrix element $M^{0\nu} = -1.57$ was found in Ref. [10] for the ground state to ground state (g.s.-to-g.s.) transition $^{150}\text{Nd} \to {}^{150}\text{Sm}$, a value substantially smaller than the recent result $M^{0\nu} = 4.74$ of Ref. [6]. In the latter publication, however, the nuclei were considered as spherical. The recent result $M^{0\nu} = -1.61$ obtained in Ref. [11] within the projected Hartree-Fock-Bogoliubov approach is in good agreement with the previous one of Ref. [10]. Also the double β decay $^{160}\text{Gd} \to {}^{160}\text{Dy}$ is of interest, although the lepton phase space factor is about one-sixth of that in the case of $^{150}\text{Nd} \to {}^{150}\text{Sm}$.

An extension of the pnQRPA method to accommodate the effect of nuclear deformation was first done in Ref. [12], where a single-particle (s.p.) basis was generated in a Nilsson potential. Further developments by including Woods-Saxon-type potentials [13], residual interactions in the particle-particle channel [14], and self-consistent deformed Hartree-Fock mean fields with consistent residual interactions [15] have followed.

Recently, the Gamow-Teller strength distributions and the $2\nu\beta\beta$-decay matrix elements have been calculated for deformed nuclei within the QRPA by making use of a phenomenological deformed Woods-Saxon potential and the schematic separable forces [16–18]. It has been found that differences in deformation between initial and final nuclei can have a pronounced effect on the $2\nu\beta\beta$-decay half-lives. However, using the schematic forces for calculating the amplitudes of the $0\nu\beta\beta$ decay would immediately raise the problem of how to fix the numerous strength parameters of the forces in different J^{π} partial channels. Therefore, using a realistic interaction with a minimal number of renormalization parameters is obviously preferable. In the present paper the approach used in Refs. [17,18] is extended to accommodate a realistic effective interaction based on the Brueckner G matrix derived from the nucleon-nucleon Bonn-CD force.

The $2\nu\beta\beta$-decay half-lives have been already measured for a dozen nuclei and the corresponding nuclear matrix elements $M^{2\nu}_{\text{exp}}$ have been extracted [19]. Theoretical interpretation of these matrix elements provides a cross-check of reliability

---

[*]vadim.rodin@uni-tuebingen.de
[†]On leave of absence from Department of Nuclear Physics, Comenius University, Mlynská dolina F1, SK-842 15 Bratislava, Slovakia.

of the calculated nuclear wave functions. In the most recent detailed spherical QRPA calculations of the $0\nu\beta\beta$-decay matrix elements Ref. [6], the renormalization parameter g_{pp} of the particle-particle residual interaction is fixed in such a way that the experimental half-lives of $2\nu\beta\beta$ decay are correctly reproduced. Thus, before calculating the matrix elements $M^{0\nu}$ by using the QRPA extended to deformed nuclei, the corresponding calculation of $M^{2\nu}$ has to be done as a test for the modeled nuclear wave functions.

II. THE QRPA IN DEFORMED NUCLEI

The inverse half-life of $2\nu\beta\beta$ decay can be expressed as a product of an accurately known phase-space factor $G^{2\nu}$ and the second-order Gamow-Teller matrix element $M^{2\nu}_{\rm GT}$ for the g.s.-to-g.s. transition [1]:

$$\left[T^{2\nu}_{1/2}(0^+_{\rm g.s.} \to 0^+_{\rm g.s.})\right]^{-1} = G^{2\nu}|M^{2\nu}_{\rm GT}|^2. \quad (1)$$

The contribution from the two successive Fermi transitions to the amplitude of the $2\nu\beta\beta$ decay can safely be neglected as it arises from isospin mixing effects (see, e.g., Ref. [2]). The double Gamow-Teller matrix element $M^{2\nu}_{\rm GT}$ in Eq. (1) can be written in the form

$$M^{2\nu}_{\rm GT} = \sum_m \frac{\langle 0^+_f \| \beta^- \| m \rangle \langle m \| \beta^- \| 0^+_i \rangle}{\bar{\omega}_m}, \quad (2)$$

where the index $i(f)$ refers to the initial (final) nuclei, the sum runs over all $|m\rangle = |1^+\rangle$ states of the intermediate odd-odd nucleus, $\beta^- = \sum_a \boldsymbol{\sigma}_a \tau^-_a$ is the Gamow-Teller transition operator, and $\bar{\omega}_m = E_m - (E_{0_i} + E_{0_f})/2 = (\omega_{m(i)} + \omega_{m(f)})/2$ with $\omega_{m(i)} = E_m - E_{0_i}$ ($\omega_{m(f)} = E_m - E_{0_f}$) representing the excitation energy of the mth state relative to the g.s. of the initial (final) nucleus.

To take into account the effect of deformation, wave functions $|1^+\rangle$ of the intermediate states in the laboratory frame that have a projection M of the total angular momentum onto the z axis can be represented in terms of wave functions in the intrinsic frame:

$$|1M(K), m\rangle = \sqrt{\frac{3}{16\pi^2}} \big[\mathcal{D}^1_{MK}(\phi, \theta, \psi) Q^\dagger_{m,K}$$
$$+ (-1)^{1+K} \mathcal{D}^1_{M-K}(\phi, \theta, \psi) Q^\dagger_{m,-K} \big] |0^+_{\rm g.s.}\rangle$$
$$(\text{for } K = \pm 1),$$

$$|1M(K), m\rangle = \sqrt{\frac{3}{8\pi^2}} \mathcal{D}^1_{MK}(\phi, \theta, \psi) Q^\dagger_{m,K} |0^+_{\rm g.s.}\rangle$$
$$(\text{for } K = 0). \quad (3)$$

Here, the correlated QRPA ground state in the intrinsic frame is denoted as $|0^+_{\rm g.s.}\rangle$, the intrinsic excitations are generated by the QRPA phonon creation operator $Q^\dagger_{m,K}$, and K is the projection of the total angular momentum onto the nuclear symmetry axis (the only projection that is conserved in strongly deformed nuclei).

These adiabatic Bohr-Mottelson-type wave functions provide an approximation that is valid for large deformations. Thus, it is well justified to treat the most interesting nuclei in question, ^{150}Nd and ^{150}Sm, which indeed are strongly

deformed, in such an approximation. The adiabatic, or the strong coupling (see, e.g., Ref. [20]), approach fails, however, for small deformations since the Coriolis force gets large and mixes states with different K. Nuclei ^{76}Ge and ^{76}Se have rather small deformations and the so-called weak-coupling, or no-alignment, limit [20] seems to be more suitable. In this limit the Coriolis force becomes so strong that the angular momenta of the valence nucleons get completely decoupled from the orientation of the core. Such a case would deserve a detailed study, which is postponed to a future publication, and the adiabatic approach to describing excited states of deformed nuclei is adopted in this present first application of the QRPA with a realistic residual interaction. Nevertheless, one might already anticipate without calculations that in the weak coupling limit the calculated observables should reveal smaller deviations from the ones obtained in the spherical limit than those calculated in the strong coupling limit of the present work. In this connection it is worth noting that spherical QRPA results can exactly be reproduced in the present calculation by letting deformation vanish, in spite of the formal inapplicability of the strong-coupling ansatz for the wave function in this limit.

The QRPA phonon creation operator acting on the ground-state wave function is given as

$$Q^\dagger_{m,K} = \sum_{pn} X^m_{pn,K} A^\dagger_{pn,K} - Y^m_{pn,K} \bar{A}_{pn,K}. \quad (4)$$

Here, $A^\dagger_{pn,K} = a^\dagger_p a^\dagger_{\bar{n}}$ and $\bar{A}_{pn,K} = a_{\bar{p}} a_n$ are the two-quasiparticle creation and annihilation operators, respectively, with the bar denoting the time-reversal operation. The quasiparticle pairs $p\bar{n}$ are defined by the selection rules $\Omega_p - \Omega_n = K$ and $\pi_p \pi_n = 1$, where π_τ is the s.p. parity and Ω_τ is the projection of the total s.p. angular momentum on the nuclear symmetry axis ($\tau = p,n$). The s.p. states $|p\rangle$ and $|n\rangle$ of protons and neutrons are calculated by solving the Schrödinger equation with the deformed axially symmetric Woods-Saxon potential [21,22]. In cylindrical coordinates the deformed Woods-Saxon s.p. wave functions $|\tau \Omega_\tau\rangle$ with $\Omega_\tau > 0$ are decomposed over the deformed harmonic oscillator s.p. wave functions [with the principal quantum numbers $(Nn_z\Lambda)$] and the spin wave functions $|\Sigma = \pm\frac{1}{2}\rangle$:

$$|\tau \Omega_\tau\rangle = \sum_{Nn_z\Sigma} b_{Nn_z\Sigma} |Nn_z\Lambda_\tau = \Omega_\tau - \Sigma\rangle |\Sigma\rangle, \quad (5)$$

where $N = n_\perp + n_z$ ($n_\perp = 2n_\rho + |\Lambda|$), n_z and n_ρ are the number of nodes of the basis functions in the z and ρ directions, respectively, and $\Lambda = \Omega - \Sigma$ and Σ are the projections of the orbital and spin angular momentum onto the symmetry axis z. For the s.p. states with the negative projection $\Omega_\tau = -|\Omega_\tau|$, which are degenerate in energy with $\Omega_\tau = |\Omega_\tau|$, the time-reversed version of Eq. (5) is used as a definition (see also Ref. [17]). The states $(\tau, \bar{\tau})$ comprise the whole single-particle model space.

The deformed harmonic oscillator wave functions $|Nn_z\Lambda\rangle$ can be further decomposed over the spherical harmonic oscillator ones $|n_r l\Lambda\rangle$ by calculating the corresponding spatial overlap integrals $A^{n_r l}_{Nn_z\Lambda} = \langle n_r l\Lambda|Nn_z\Lambda\rangle$ (where n_r is the radial quantum number and l and Λ are the orbital angular

momentum and its projection onto z axes, respectively). (See the Appendix for the details.) Thereby, the wave function [Eq. (5)] can be reexpressed as

$$|\tau\Omega_\tau\rangle = \sum_\eta B_\eta^\tau |\eta\Omega_\tau\rangle, \qquad (6)$$

where $|\eta\Omega_\tau\rangle = \sum_\Sigma C_{l\Omega_\tau - \Sigma \frac{1}{2}\Sigma}^{j\Omega_\tau}|n_r l \Lambda = \Omega_\tau - \Sigma\rangle|\Sigma\rangle$ is the spherical harmonic oscillator wave function in the j-coupled scheme $[\eta = (n_r l j)]$, and $B_\eta^\tau = \sum_\Sigma C_{l\Omega_\tau - \Sigma \frac{1}{2}\Sigma}^{j\Omega_\tau} A_{N n_z \Omega_\tau - \Sigma}^{n_r l} b_{N n_z \Sigma}$, with $C_{l\Omega_\tau - \Sigma \frac{1}{2}\Sigma}^{j\Omega_\tau}$ being the Clebsch-Gordan coefficient.

The QRPA equations

$$\begin{pmatrix} \mathcal{A}(K) & \mathcal{B}(K) \\ -\mathcal{B}(K) & -\mathcal{A}(K) \end{pmatrix} \begin{pmatrix} X_K^m \\ Y_K^m \end{pmatrix} = \omega_{K,m} \begin{pmatrix} X_K^m \\ Y_K^m \end{pmatrix}, \qquad (7)$$

with realistic residual interaction, are solved to get the forward X_{iK}^m and backward Y_{iK}^m amplitudes and the excitation energies $\omega_K^{m_i}$ and $\omega_K^{m_f}$ of the mth K^+ ($K = 0, \pm 1$) state in the intermediate nucleus. The matrices $\mathcal{A}$ and $\mathcal{B}$ are defined by

$$\begin{aligned} \mathcal{A}_{pn,p'n'}(K) &= \delta_{pn,p'n'}(E_p + E_n) + g_{pp}(u_p u_n u_{p'} u_{n'} \\ &\quad + v_p v_n v_{p'} v_{n'})V_{p\bar{n}p'\bar{n}'} - g_{ph}(u_p v_n u_{p'} v_{n'} \\ &\quad + v_p u_n v_{p'} u_{n'})V_{pn'p'n}, \qquad (8) \\ \mathcal{B}_{pn,p'n'}(K) &= -g_{pp}(u_p u_n v_{p'} v_{n'} + v_p v_n u_{p'} u_{n'})V_{p\bar{n}p'\bar{n}'} \\ &\quad - g_{ph}(u_p v_n v_{p'} u_{n'} + v_p u_n u_{p'} v_{n'})V_{pn'p'n}, \end{aligned}$$

where $E_p + E_n$ are the two-quasiparticle excitation energies, $V_{pn,p'n'}$ and $V_{p\bar{n},p'\bar{n}'}$ are the p-h and p-p matrix elements of the residual nucleon-nucleon interaction V, respectively, and u_τ and v_τ are the coefficients of the Bogoliubov transformation. The amplitudes of β^- and β^+ transitions from the 0^+ ground states of initial and final nuclei to a one-phonon K^+ state in the intermediate nucleus are given in the intrinsic system by

$$\langle K^+, m|\beta_K^-|0_{\text{g.s.}}^+\rangle = \sum_{pn}\langle p|\sigma_K|n\rangle[u_p v_n X_{pn,K}^m + v_p u_n Y_{pn,K}^m],$$
$$(9)$$
$$\langle K^+, m|\beta_K^+|0_{\text{g.s.}}^+\rangle = \sum_{pn}\langle p|\sigma_K|n\rangle[u_p v_n Y_{pn,K}^m + v_p u_n X_{pn,K}^m].$$

The matrix element $M_{\text{GT}}^{2\nu}$ of Eq. (2) is given within the QRPA in the intrinsic system by the following expression:

$$\begin{aligned} M_{\text{GT}}^{2\nu} &= \sum_{K=0,\pm 1}\sum_{m_i m_f} \\ &\quad \times \frac{\langle 0_f^+|\bar{\beta}_K^-|K^+, m_f\rangle\langle K^+, m_f|K^+, m_i\rangle\langle K^+, m_i|\beta_K^-|0_i^+\rangle}{\bar{\omega}_{K,m_i m_f}}. \end{aligned}$$
$$(10)$$

Along with the usual approximation of the energy denominator in Eq. (10) as $\bar{\omega}_{K,m_i m_f} = (\omega_{K,m_f} + \omega_{K,m_i})/2$ (see, e.g., Refs. [17,18]; we will later refer to this case as "case II"), we also use in this work another prescription in which the whole calculated QRPA energy spectrum is shifted in such a way as to have the first calculated 1^+ state exactly at the corresponding experimental energy (case I). In this case the energy denominator in Eq. (10) acquires the form $\bar{\omega}_{K,m_i m_f} = (\omega_{K,m_f} - \omega_{K,1_f} + \omega_{K,m_i} - \omega_{K,1_i})/2 + \bar{\omega}_{1_1^+}$, with $\bar{\omega}_{1_1^+}$ being

the experimental excitation energy of the first 1^+ state measured from the mean g.s. energy $(E_{0_i} + E_{0_f})/2$. All the calculated strength functions in this work are represented according to case I, as well.

The two sets of intermediate nuclear states generated from the initial and final ground states do not come out identical within the QRPA. Therefore, the overlap factor of these states is introduced in Eq. (10) [23,24] as follows:

$$\begin{aligned} \langle K^+, m_f|K^+, m_i\rangle &= \sum_{l_i l_f}\left[X_{l_f K}^{m_f} X_{l_i K}^{m_i} - Y_{l_f K}^{m_f} Y_{l_i K}^{m_i}\right] \\ &\quad \times \mathcal{R}_{l_f l_i}\langle BCS_f|BCS_i\rangle. \end{aligned} \qquad (11)$$

The factor $\mathcal{R}_{l_f l_i}$, which includes the overlaps of single-particle wave functions of the initial and final nuclei, is given by

$$\begin{aligned} \mathcal{R}_{ll'} &= \langle p\rho_p|p'\rho_{p'}\rangle\big(u_p^{(i)}u_{p'}^{(f)} + v_p^{(i)}v_{p'}^{(f)}\big)\langle n\rho_n|n'\rho_{n'}\rangle \\ &\quad \times \big(u_n^{(i)}u_{n'}^{(f)} + v_n^{(i)}v_{n'}^{(f)}\big), \end{aligned} \qquad (12)$$

and the last term $\langle BCS_f|BCS_i\rangle$ in Eq. (11) corresponds to the overlap factor of the initial and final BCS vacua in the form given in Ref. [17].

As a residual two-body interaction we use the nuclear Brueckner G matrix, which is a solution of the Bethe-Goldstone equation, derived from the Bonn-CD one-boson exchange potential, as used also in the spherical calculations of Ref. [6]. The G-matrix elements are originally calculated with respect to a spherical harmonic oscillator s.p. basis. By using the decomposition of the deformed s.p. wave function in Eq. (6), the two-body deformed wave function can be represented as

$$|p\bar{n}\rangle = \sum_{\eta_p \eta_n J} F_{p\eta_p n\eta_n}^{JK}|\eta_p\eta_n, JK\rangle, \qquad (13)$$

where $|\eta_p\eta_n, JK\rangle = \sum_J C_{j_p\Omega_p j_n\Omega_n}^{JK}|\eta_p \Omega_p\rangle|\eta_n\Omega_n\rangle$, and $F_{p\eta_p n\eta_n}^{JK} = B_{\eta_p}^p B_{\eta_n}^n (-1)^{j_n - \Omega_n} C_{j_p\Omega_p j_n - \Omega_n}^{JK}$ is defined for the sake of simplicity [with the phase $(-1)^{j_n - \Omega_n}$ arising from the time-reversed states $|\bar{n}\rangle$]. The particle-particle $V_{p\bar{n},p'\bar{n}'}$ and particle-hole $V_{pn',p'n}$ interaction matrix elements in the representation [Eq. (8)] for the QRPA matrices $\mathcal{A}$ and $\mathcal{B}$ [Eq. (7)] in the deformed Woods-Saxon single-particle basis can then be given in terms of the spherical G-matrix elements as follows:

$$\begin{aligned} V_{p\bar{n},p'\bar{n}'} &= -2\sum_J \sum_{\eta_p \eta_n}\sum_{\eta_{p'}\eta_{n'}} F_{p\eta_p n\eta_n}^{JK} F_{p'\eta_{p'} n'\eta_{n'}}^{JK} \\ &\quad \times G(\eta_p\eta_n\eta_{p'}\eta_{n'}, J), \end{aligned} \qquad (14)$$

$$\begin{aligned} V_{pn',p'n} &= 2\sum_J \sum_{\eta_p \eta_n}\sum_{\eta_{p'}\eta_{n'}} F_{p\eta_p \bar{n}'\eta_{n'}}^{JK'_{pn'}} F_{p'\eta_{p'}\bar{n}\eta_n}^{JK'_{pn'}} \\ &\quad \times G(\eta_p\eta_{n'}\eta_{p'}\eta_n, J), \end{aligned} \qquad (15)$$

where $K'_{pn'} = \Omega_p + \Omega_{n'} = \Omega_{p'} + \Omega_n$. The matrix elements of σ_K in Eq. (9) can be written as $\langle p|\sigma_K|n\rangle = \sum_{\eta_p,\eta_n} F_{p\eta_p n\eta_n}^{1K}$ $\langle \eta_p\|\sigma\|\eta_n\rangle/\sqrt{3}$.

TABLE I. The values of the deformation parameter β_2 for initial (final) nuclei adopted in the calculations along with the fitted values of the p-p strength parameters g_{pp} (for the realistic Bonn-CD force) and κ (for a phenomenological separable force) for two ways of calculating $M_{\mathrm{GT}}^{2\nu}$, (I) and (II). The p-h strength parameters $g_{ph} = 1.15$ and $\chi = 3.73/A^{0.7}$ MeV are fixed as explained in the text. In the last column the calculated (with the Bonn-CD force) values of the Ikeda sum rule [in percentage of $3(N-Z)$] are given for the initial (final) nucleus.

Nucleus	β_2	g_{pp} (I)	g_{pp} (II)	κ (I) (MeV)	κ (II) (MeV)	ISR (%)
^{76}Ge (^{76}Se)	0.0 (0.0)	0.94	0.91	0.087	0.083	96.8 (98.2)
	0.10 (0.16) [25]	0.99	0.97	0.091	0.088	96.1 (96.8)
^{150}Nd (^{150}Sm)	0.0 (0.0)	1.11	1.11	0.051	0.050	94.8 (95.9)
	0.37 (0.23) [25]	0.78	0.65	0.033	0.005	94.1 (95.8)
	0.24 (0.21) [26]	1.35	1.32	0.053	0.052	95.4 (96.2)

III. RESULTS

The Gamow-Teller strength distributions and the $2\nu\beta\beta$-decay amplitudes for the g.s.-to-g.s. transitions are calculated for the nuclear systems with $A = 76$ (^{76}Ge $\rightarrow$ ^{76}Se) and $A = 150$ (^{150}Nd $\rightarrow$ ^{150}Sm). The single-particle Schrödinger equation with the Hamiltonian of a deformed Woods-Saxon mean field [21,22] is solved on the basis of an axially deformed harmonic oscillator [see Eq. (5)]. The s.p. basis corresponding in the spherical limit to full $(2-4)\hbar\omega$ major oscillator shells for the nuclei with $A = 76$ and $(4-6)\hbar\omega$ for $A = 150$ are used. Decomposition over the states within seven major spherical harmonic oscillator shells is done in Eq. (13). Only quadrupole deformation is taken into account in the calculations. The deformation parameter β_2 is obtained as $\beta_2 = \sqrt{\frac{\pi}{5}} \frac{Q_p}{Z r_c^2}$ (where r_c is the charge rms radius) by using the empirical intrinsic quadrupole moments Q_p, which are derived from the laboratory quadrupole moments measured by the Coulomb excitation reorientation technique [25]. The corresponding values of β_2 are listed in Table I. The spherical limit (i.e., $\beta_2 = 0$) is considered in all cases as well. Because of the rather large experimental errors $\beta_2 = 0.37 \pm 0.09$ and $\beta_2 = 0.23 \pm 0.03$ [25] for ^{150}Nd and ^{150}Sm, respectively, we also adopt for these nuclei the respective calculated values from Ref. [26], which seem to fit better the rotational bands in these nuclei.

First, the BCS equations are solved self-consistently to obtain the occupation amplitudes u_τ and v_τ, gap parameter Δ_τ, and the chemical potentials λ_p and λ_n [27]. The renormalizing strengths g_{pair}^p and g_{pair}^n of the proton and neutron pairing interactions are determined to reproduce the experimental pairing energies through a symmetric five-term formula [28].

For calculating the QRPA energies and wave functions one has to fix the particle-hole g_{ph} and particle-particle g_{pp} renormalization factors of the residual interaction in Eq. (8). An appropriate value of g_{ph} can be determined by reproducing the experimental position of the Gamow-Teller giant resonance (GTR) in the intermediate nucleus, whereas the parameter g_{pp} can be determined from fitting the experimental value $M_{\mathrm{exp}}^{2\nu}$. The experimental energy position of the GTR relative to the energy of the first excited 1^+ state in ^{76}Ge can be reproduced with $g_{ph} = 1.15$ [where the prescription of case I is used; see the explanation after Eq. (10)]. Since there is no experimental information on the GTR energy for ^{150}Nd, we use

for this nucleus the same $g_{ph} = 1.15$. Two sets of parameters g_{pp} obtained from fitting $M_{\mathrm{exp}}^{2\nu}$ in two calculations of $M_{\mathrm{GT}}^{2\nu}$ (case I and case II) are listed in Table I. The difference between g_{pp} fitted in case I and case II is usually quite small. To compare with the previous QRPA results, we have performed calculations also with the separable p-h and p-p interactions in a way similar to what was done in Refs. [17,18]. The coefficient in the A dependence of the p-h strength parameter $\chi = 3.73/A^{0.7}$ MeV is fitted to reproduce the GTR energy in ^{76}Ge and is used then in the calculations for ^{150}Nd (with the form of the A dependence taken from Ref. [14]). The corresponding fitted values of the strength parameters κ of the separable p-p interaction are also listed in Table I. All the calculations in this work are done with the mean-field spin-orbit coupling constant increased by a factor of 1.2 as compared with the one used in Refs. [17,18], which gives a better correspondence with the parametrization of the spherical Woods-Saxon mean field used in Ref. [6]. Therefore, we get slightly different fitted values of χ and κ as compared with Refs. [17,18].

The calculation of single β^- and β^+ decay branches for parent and daughter nuclei is the starting point for the calculation of the $2\nu\beta\beta$-decay amplitudes. The calculated Gamow-Teller strength distributions for all the nuclei in question are shown in Figs. 1 and 2 as functions of the excitation energy in the intermediate (for the $2\nu\beta\beta$ decay) nuclei. The representation is according to the convention of case I (i.e., the entire calculated GT spectrum is shifted to fit the experimental energy of the first 1^+ state). To facilitate comparison among various calculations the Gamow-Teller distributions are smoothed with a Gaussian of width 1 MeV, so the original discrete spectrum of $B(GT)$ values is transformed into a continuous one of the strength function $S(GT)$. The relevant strength distributions for the double β decay are the $S(GT^-)$ one for the parent nucleus (two upper panels) and the $S(GT^+)$ distribution for the daughter nucleus (two lower panels). In the left panels (labeled "Realistic") the results obtained by using a realistic nucleon-nucleon interaction (Bonn-CD force) are shown; the right panels (labeled "Separable") show the results obtained by using a separable interaction of Ref. [18]. In both types of calculations the corresponding strengths of the p-h interaction g_{ph} and χ are fixed by fitting the experimental energy of the Gamow-Teller resonance in ^{76}Ge as described in the preceding paragraph. The thick solid and the dashed lines represent the
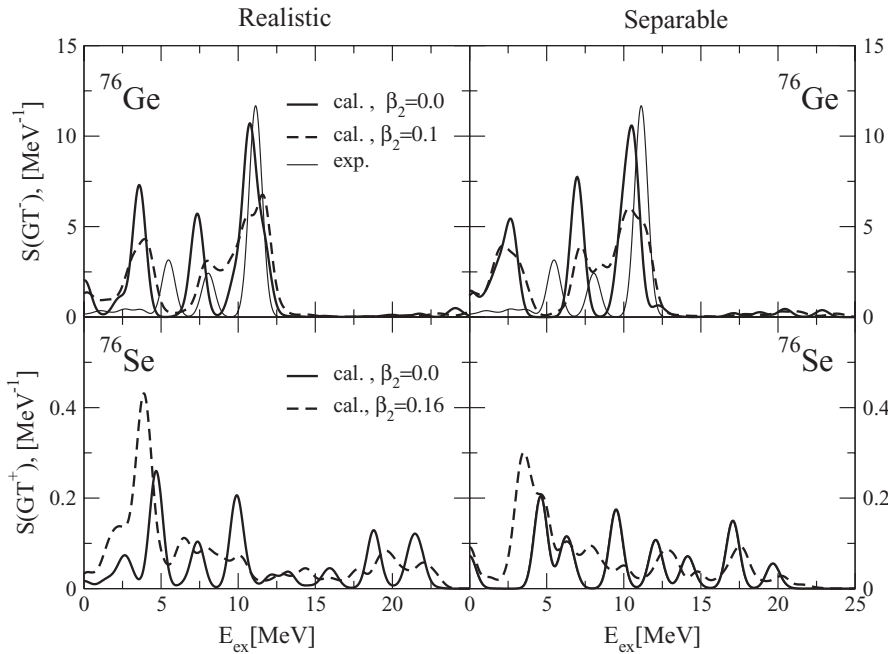
FIG. 1. Gamow-Teller strength distributions $S(GT^-)$ in ^{76}Ge and $S(GT^+)$ in ^{76}Se as functions of the excitation energy E_{ex} in the intermediate (for ^{76}Ge $\rightarrow$ ^{76}Se decay) nucleus ^{76}As. The QRPA calculation results obtained with realistic and separable forces are shown in the left and right panels, respectively. (Upper panels) The results corresponding to the spherical ($\beta_2 = 0.0$) and deformed ($\beta_2 = 0.1$) ground state of ^{76}Ge are represented by the thick solid and dashed lines, respectively. Experimental data (thin solid line) are from Ref. [29]. (Lower panels) The results corresponding to the spherical ($\beta_2 = 0.0$) and deformed ($\beta_2 = 0.16$) ground state of ^{76}Se are represented by the thick solid and dashed lines, respectively.

results obtained in the spherical limit $\beta_2 = 0$ and with the realistic deformation, respectively. The thin solid line in Fig. 1 represents the Gaussian-smeared experimental $B(GT)$ values for ^{76}Ge taken from Ref. [29].

In the case of the β^- distribution, one observes that the position of the Gamow-Teller resonance is not sensitive to the effect of deformation. For the β^+ distribution, the effect of deformation is more apparent in the strength distribution than that in the case of the β^- one. Comparing the results obtained with the realistic and schematic residual interaction one can see some marked differences in the β^+ and the low-energy part of the β^- strength distributions. The Ikeda sum rule is underestimated by a small amount (about 3%–5%) in the calculations (see the last column of Table I; to get 100%

one would need to have the whole s.p. basis, as is done, for instance, within the continuum-QRPA; see, e.g., Ref. [30]). This also means that the chosen s.p. model spaces (see the beginning of this section) are large enough.

Figure 3 illustrates the evolution of the strength functions $S(GT^-)$ in ^{76}Ge and ^{150}Nd with respect to an increase of g_{pp} in the spherical limit ($\beta_2 = 0$). One can see in the figure that all the GT peaks get shifted to smaller energies as g_{pp} increases. In addition, the low-lying GT states become more collective and, correspondingly, the low-energy part of the GT strength gets markedly larger at the expense of a decrease in the GTR strength. It can also be seen that the QRPA calculations with the realistic g_{pp} values as listed in Table I are still quite far from the collapse of the QRPA. One may argue that the results show
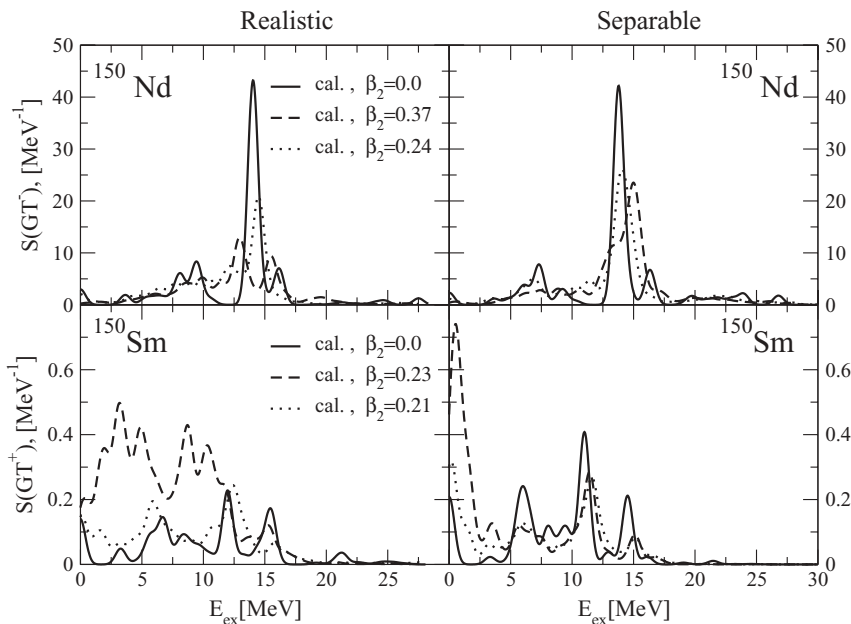
FIG. 2. The same as in Fig. 1, but for ^{150}Nd and ^{150}Sm.
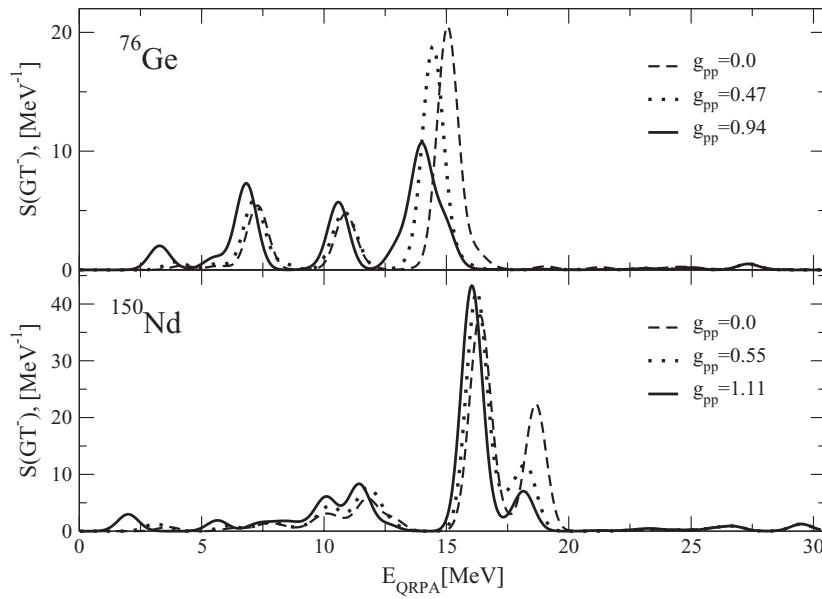
FIG. 3. Gamow-Teller strength distributions $S(GT^-)$ in ^{76}Ge and ^{150}Nd (spherical limit) for different particle-particle interaction strengths g_{pp} as functions of the QRPA energy E_{QRPA}. The solid lines (the same as in the upper left panels of Figs. 1 and 2) represent $S(GT^-)$ corresponding to the fitted g_{pp} (Table I). The dashed and the dotted lines correspond to smaller g_{pp} as indicated in the figure.

a low-energy part of the GT spectrum that is too enhanced as compared with the experiment. This discrepancy might have to do with the neglect of quenching in the present calculation. For $g_A < 1.25$ the corresponding experimental value of $M_{\exp}^{2\nu}$ gets larger and a smaller g_{pp} would be needed to fit it. This effect deserves a separate detailed study, similar to the one performed in Ref. [31], which lies outside the scope of the present work.

As shown in Refs. [17,18], deformation introduces a mechanism of suppression of the $M_{GT}^{2\nu}$ matrix element that works even for the same initial and final deformations. The reduction gets even stronger when initial and final deformations differ from each other and is mainly due to a decrease of the BCS overlap [Eq. (11)]. The values of the overlap calculated with the realistic pairing interaction are very close to those

obtained by using the constant pairing gap as in Refs. [17,18], which is illustrated in Fig. 4 for the transition ^{76}Ge $\rightarrow$ ^{76}Se. In addition, there is the well-known reduction of the values of $M_{GT}^{2\nu}$ with increasing renormalization parameter g_{pp} of the p-p interaction [6,7]. It is interesting to study all these suppression mechanisms within the QRPA with the realistic residual interaction that is the main thrust of this work.

The calculated matrix elements $M_{GT}^{2\nu}$ are shown in Figs. 5 and 6 as functions of the parameter g_{pp} and for different deformations of initial and final nuclei. The parameters β_2, g_{ph}, and χ used are the same as in the study of the Gamow-Teller distributions. Again, in the left panels (labeled "Realistic") the results of the present work using the realistic nucleon-nucleon interaction (Bonn-CD force) are shown and in the right panels (labeled "Separable") the results using separable interaction
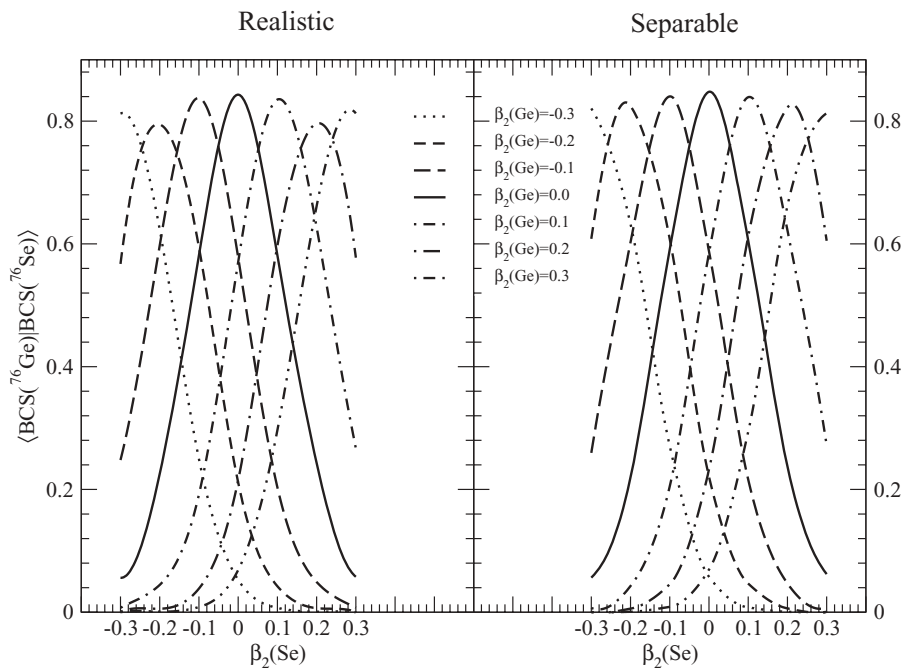
FIG. 4. The dependence of the BCS overlap factor in Eq. (11) on the difference in deformations of ^{76}Ge and ^{76}Se. The calculation results obtained with realistic and separable forces are shown in the left and right panels, respectively.
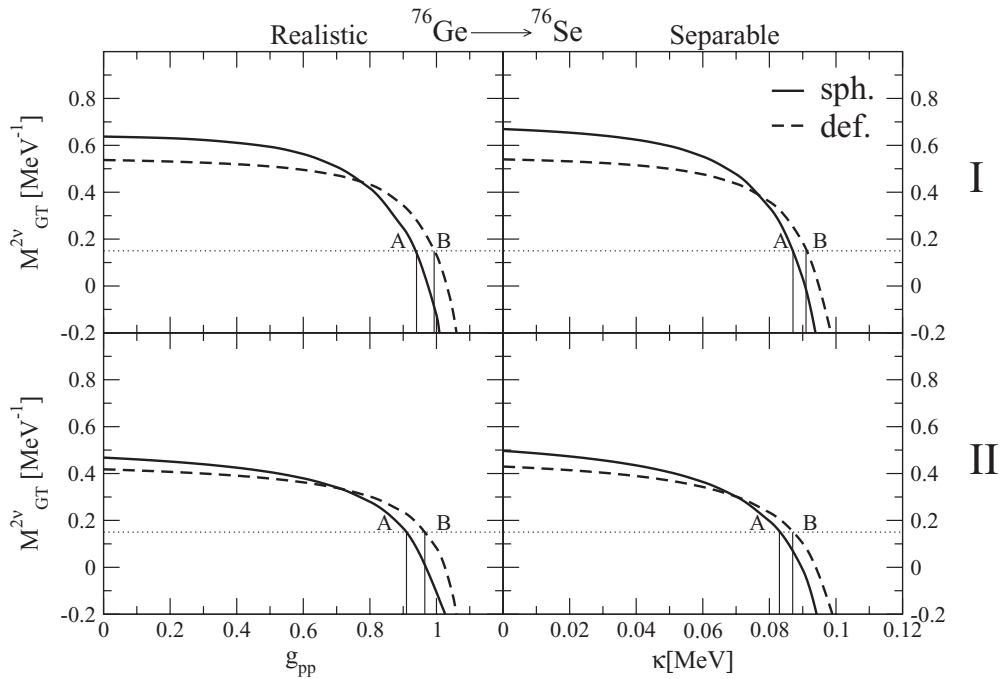
FIG. 5. $2\nu\beta\beta$-decay matrix element for ^{76}Ge $\rightarrow$ ^{76}Se decay as functions of particle-particle interaction strength g_{pp} of the realistic forces (left panels) and of κ of the separable forces (right panels). The solid line ("sph.") corresponds to spherical shape of the initial and final nuclei. The dashed one ("def.") is associated with the deformation parameters taken from Ref. [25] [$\beta_2(^{76}$Ge$) = 0.1$, $\beta_2(^{76}$Se$) = 0.16$]. The dotted horizontal line corresponds to experimental $M^{2\nu}_{\exp}$ obtained in Ref. [19] using $g_A = 1.25$. The points A and B in each panel specify the values of the p-p interaction for which the value of $M^{2\nu}_{\exp}$ is fitted. The upper (case I) and lower (case II) panels correspond to the calculations with the shifted and unshifted QRPA spectrum, respectively, as explained in the text.

are presented. The upper panels represent the results obtained with the shifted calculated QRPA spectrum [case I; see the explanation after Eq. (10)] and in the lower ones the results obtained with the usual unshifted QRPA spectrum (case II) are shown. The solid lines in Figs. 5 and 6 represent the

matrix elements $M^{2\nu}_{\rm GT}$ calculated in the spherical limit whereas the dashed ones (and dot-dashed in Fig. 6) represent $M^{2\nu}_{\rm GT}$ calculated for realistic deformations. The dotted horizontal line corresponds to the corresponding experimental $M^{2\nu}_{\exp}$ values obtained in Ref. [19] by using the unquenched value of the
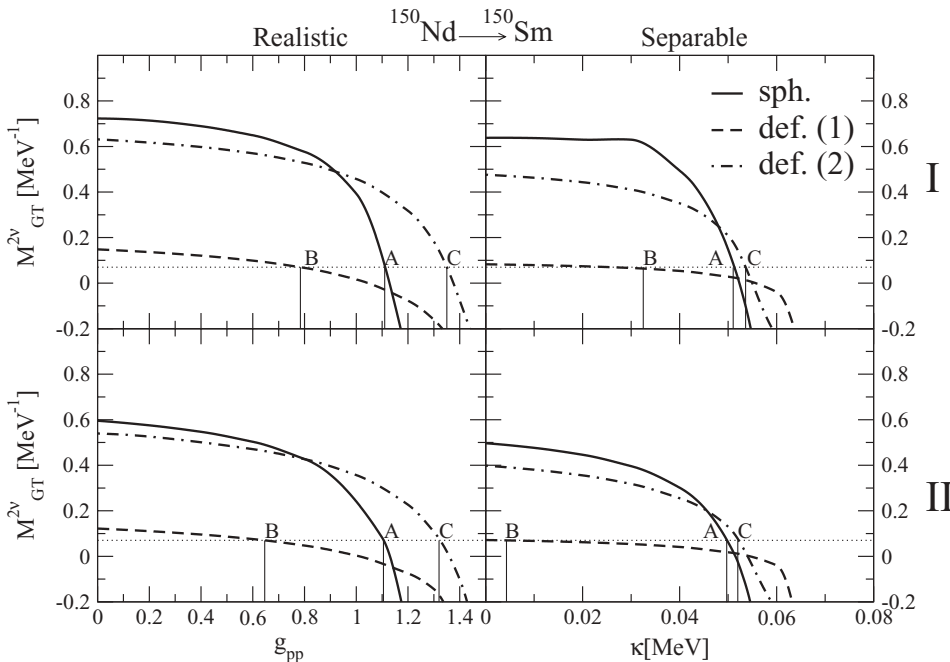
FIG. 6. The same as in Fig. 5, but for ^{150}Nd $\rightarrow$ ^{150}Sm decay with two different sets of deformation parameters: from Ref. [25] [$\beta_2(^{150}$Nd$) = 0.37$, $\beta_2(^{150}$Sm$) = 0.23$, "def. (1)"] and from Ref. [26] [$\beta_2(^{150}$Nd$) = 0.24$, $\beta_2(^{150}$Sm$) = 0.21$, "def. (2)"].

axial-vector coupling constant $g_A = 1.25$. The points A and B (and C for $^{150}\text{Nd} \to {}^{150}\text{Sm}$) in each panel specify the values of the p-p interaction for which the value of $M_{\text{exp}}^{2\nu}$ is reproduced for spherical and deformed cases, respectively (with the corresponding values of g_{pp} and κ listed in Table I). The calculated $M_{\text{GT}}^{2\nu}$ decreases faster in the spherical case than in the deformed one as g_{pp} increases, and the fitted value of g_{pp} is usually larger in the case of deformation than that for the spherical limit. Another interesting feature is that for nonzero deformation the calculated $M_{\text{GT}}^{2\nu}$ is smaller at $g_{pp} = 0$ than those in the spherical limit, in agreement with the previous results of Refs. [17,18]. This suppression already holds when initial and final nuclei are equally deformed and gets stronger with increasing difference in deformation between initial and final nuclei (as the BCS overlap plays an important role in the reduction of $M_{GT}^{2\nu}$, as discussed in Refs. [17,18]). It is also worth mentioning that the calculated $M_{\text{GT}}^{2\nu}$ for the $^{150}\text{Nd} \to {}^{150}\text{Sm}$ transition (Fig. 6) comes out rather small when the experimental deformation parameters from Ref. [25] are used, whereas by using the deformation parameters of Ref. [26] the corresponding $M_{\text{exp}}^{2\nu}$ can be fitted for a reasonable value of g_{pp}. Also, the values of $M_{\text{GT}}^{2\nu}$ calculated with the shifted QRPA spectrum, though a little bit larger at $g_{pp} \ll 1$ than the unshifted ones, fit the corresponding experimental values at almost the same g_{pp} (see Table I).

IV. CONCLUSIONS

In the present work the two-neutrino double β decay (g.s.-to-g.s. transitions) and relevant Gamow-Teller strength distributions are calculated within the QRPA for the nuclear systems $^{76}\text{Ge} \to {}^{76}\text{Se}$ and $^{150}\text{Nd} \to {}^{150}\text{Sm}$ by taking into account effects of nuclear deformation. For the first time a realistic residual two-body interaction based on the Brueckner G matrix (for the Bonn-CD force) is implemented in deformed calculations. The G-matrix elements in the deformed Wood-Saxon basis are calculated by expanding the deformed single-particle wave functions over the spherical harmonic oscillator ones. The effect of deformation on the observables is studied within this framework. The suppression of the calculated $M_{\text{GT}}^{2\nu}$, resulting from both nonzero deformation and the interaction in the particle-particle channel, is observed, in accordance with previous calculations with separable forces [17,18]. The present work marks the first important step toward using QRPA calculations of the neutrinoless double β decay of deformed nuclei such as ^{150}Nd with a realistic nucleon-nucleon interaction.

APPENDIX: CALCULATION OF THE OVERLAP INTEGRALS

In this Appendix we describe how the deformed harmonic oscillator wave functions can be decomposed over the spher-

ical ones by calculating the corresponding spatial overlap integrals.

The normalized wave equation of the three-dimensional axially deformed harmonic oscillator in cylindrical coordinates (ρ, z, ϕ) are given by a product of three functions:

$$|Nn_z\Lambda\rangle = \psi_{n_\rho}^{|\Lambda|}(\rho)\psi_{n_z}(z)\frac{e^{i\Lambda\phi}}{\sqrt{2\pi}}, \qquad (A1)$$

where Λ is the projection of the orbital angular momentum on the z (symmetry) axis and N is the principal quantum number, which is defined as $N = n_z + 2n_\rho + |\Lambda|$. The radial function $\psi_{n_\rho}^{|\Lambda|}$ is usually written in terms of a dimensionless coordinate η as

$$\psi_{n_\rho}^{|\Lambda|}(\rho) = C_{n_\rho}^{|\Lambda|}\eta^{\frac{|\Lambda|}{2}}e^{-\frac{\eta}{2}}L_{n_\rho}^{|\Lambda|}(\eta), \qquad (A2)$$

with $\eta = \frac{\rho^2}{b_\perp^2}$, where $b_\perp = \sqrt{\frac{\hbar}{m\omega_\perp}}$ is the oscillator length for the motion perpendicular to the z axis, $C_{n_\rho}^{|\Lambda|} = (\frac{2n_\rho!}{(n_\rho+|\Lambda|)!b_\perp^2})^{\frac{1}{2}}$ is a normalization factor, and $L_{n_\rho}^{|\Lambda|}(\eta)$ are the associated Laguerre polynomials. The z-dependent function ψ_{n_z} is similarly written in terms of a dimensionless variable ξ as

$$\psi_{n_z}(z) = C_{n_z}e^{-\frac{\xi^2}{2}}H_{n_z}(\xi), \qquad (A3)$$

with $\xi = \frac{z}{b_z}$, where b_z is oscillator length in the direction of the z axis, $C_{n_z} = (\sqrt{\pi}2^{n_z}n_z!b_z)^{-\frac{1}{2}}$ is a normalization factor, and $H_{n_z}(\xi)$ are the Hermite polynomials.

The normalized wave functions of the three-dimensional isotropic harmonic oscillator in spherical polar coordinates (r,θ,ϕ) are given as

$$|Nl\Lambda\rangle = \psi_{n_r l}(r)Y_{l\Lambda}(\theta, \phi), \qquad (A4)$$

where n_r is the radial quantum number, $Y_{l\Lambda}$ is the spherical harmonic, and l is the orbital angular momentum. The radial part $\psi_{n_r l}$ is written in terms of a dimensionless coordinate ν as

$$\psi_{n_r}^l(r) = C_{n_r l}\nu^{l/2}e^{-\frac{\nu}{2}}L_{n_r}^{(l+\frac{1}{2})}(\nu), \qquad (A5)$$

with $\nu = \frac{r^2}{b_0^2}$, where b_0 is the spherical oscillator length, $C_{n_r l} = (\frac{2n_r!}{(n_r+l+\frac{1}{2})!b_0^3})^{\frac{1}{2}}$ is a normalization factor, and $L_{n_r}^{(l+\frac{1}{2})}(\nu^2)$ are the associated Laguerre polynomials.

The wave functions $|Nn_z\Lambda\rangle$ of the deformed harmonic oscillator can be decomposed over the spherical ones $|Nl\Lambda\rangle$ as

$$|Nn_z\Lambda\rangle = \sum_{n_r l\Lambda} A_{Nn_z\Lambda}^{Nl}|Nl\Lambda\rangle, \qquad (A6)$$

where $A_{Nn_z\Lambda}^{Nl} = \langle Nl\Lambda|Nn_z\Lambda\rangle$ is the spatial overlap integral, which can be numerically calculated in the spherical coordinate system as follows:

$$A_{Nn_z\Lambda}^{Nl}$$
$$= \sqrt{2\pi}\int_0^\infty \left(\int_0^\pi \psi_{n_\rho}^{|\Lambda|}(r\sin\theta)\psi_{n_z}(r\cos\theta)\right.$$
$$\left. \times Y_{l\Lambda}^*(\theta, \phi = 0)\sin\theta d\theta\right)\psi_{n_r l}(r)r^2 dr. \qquad (A7)$$

[1] F. Boehm and P. Vogel, *Physics of Massive Neutrinos* (Cambridge University Press, Cambridge, UK, 1992).

[2] W. C. Haxton and G. S. Stephenson, Prog. Part. Nucl. Phys. **12**, 409 (1984).

[3] A. Faessler and F. Šimkovic, J. Phys. G **24**, 2139 (1998).

[4] O. Civitarese and J. Suhonen, Phys. Rep. **300**, 123 (1998).

[5] J. A. Halbleib and R. A. Sorensen, Nucl. Phys. **A98**, 542 (1967).

[6] V. A. Rodin, A. Faessler, F. Šimkovic, and P. Vogel, Phys. Rev. C **68**, 044302 (2003); Nucl. Phys. **A766**, 107 (2006); **A793**, 213(E) (2007).

[7] P. Vogel and M. R. Zirnbauer, Phys. Rev. Lett. **57**, 3148 (1986); D. Cha, Phys. Rev. C **27**, 2269 (1983); T. Tomoda and A. Faessler, Phys. Lett. **B199**, 475 (1987); K. Muto, E. Bender, and H. V. Klapdor, Z. Phys. A **334**, 177 (1989).

[8] K. Zuber (SNO+ Collaboration), Proc. MEDEX'07, Prague, Czech Republic, 11–14 June 2007; AIP Conf. Proc. **942**, 101 (2007).

[9] L. Simard (SuperNEMO Collaboration), Proc. MEDEX'07, Prague, Czech Republic, 11–14 June 2007; AIP Conf. Proc. **942**, 72 (2007).

[10] J. G. Hirsch, O. Castanos, and O. Hess, Nucl. Phys. **A582**, 124 (1995).

[11] K. Chaturvedi, R. Chandra, P. K. Rath, P. K. Raina, and J. G. Hirsch, arXiv:0805.4073 [nucl-th].

[12] J. Krumlinde and P. Moeller, Nucl. Phys. **A417**, 419 (1984).

[13] P. Moeller and J. Randrup, Nucl. Phys. **A514**, 1 (1990).

[14] H. Homma, E. Bender, M. Hirsch, K. Muto, H. V. Klapdor-Kleingrothaus, and T. Oda, Phys. Rev. C **54**, 2972 (1996).

[15] P. Sarriguren, E. Moya de Guerra, A. Escuderos, and A. C. Carrizo, Nucl. Phys. **A635**, 55 (1998); P. Sarriguren, E. Moya de Guerra, and A. Escuderos, *ibid.* **A658**, 13 (1999); **A691**, 631 (2001); Phys. Rev. C **64**, 064306 (2001).

[16] P. Sarriguren, E. Moya de Guerra, L. Pacearescu, A. Faessler, F. Šimkovic, and A. A. Raduta, Phys. Rev. C **67**, 044313 (2003).

[17] F. Šimkovic, L. Pacearescu, and A. Faessler, Nucl. Phys. A **733**, 321 (2004).

[18] R. Alvarez-Rodriguez, P. Sarriguren, E. Moya de Guerra, L. Pacearescu, A. Faessler, and F. Šimkovic, Phys. Rev. C **70**, 064309 (2004).

[19] A. S. Barabash, Czech. J. Phys. **50**, 437 (2006).

[20] P. Ring and P. Schuck, *The Nuclear Many Body Problem* (Springer-Verlag, Berlin, 1980).

[21] J. Damgaard, Pauli, V. V. Pashkevich, and V. M. Strutinski, Nucl. Phys. **A135**, 432 (1969).

[22] R. Nojarov, Z. Bochnacki, and A. Faessler, Z. Phys. A **324**, 289 (1986).

[23] F. Šimkovic, G. Pantis, and A. Faessler, Prog. Part. Nucl. Phys. **40**, 285 (1998); Phys. At. Nucl. **61**, 1218 (1998).

[24] W. A. Kaminski and A. Faessler, Nucl. Phys. **A529**, 605 (1991).

[25] P. Raghavan, At. Data Nucl. Data Tables **42**, 189 (1989).

[26] P. Moeller, J. R. Nix, W. D. Myers, and W. J. Swiatecki, At. Data Nucl. Data Tables **59**, 185 (1995).

[27] M. S. Yousef, V. Rodin, and A. Faessler, Prog. Part. Nucl. Phys. **59**, 494 (2007).

[28] G. Audi and A. H. Wapstra, Nucl. Phys. **A729**, 337 (2003).

[29] R. Madey, B. S. Flanders, B. D. Anderson, A. R. Baldwin, J. W. Watson, S. M. Austin, C. C. Foster, H. V. Klapdor, and K. Grotz, Phys. Rev. C **40**, 540 (1989).

[30] V. Rodin and A. Faessler, Phys. Rev. C **77**, 025502 (2008).

[31] A. Faessler, G. L. Fogli, E. Lisi, V. Rodin, A. M. Rotunno, and F. Simkovic, J. Phys. G **35**, 075104 (2008).